ELSEVIER

Journal of Fluids and Structures 19 (2004) 933–941

JOURNAL OF FLUIDS AND STRUCTURES

www.elsevier.nl/locate/jnlabr/yjfls

Effects of compliant coatings on radiated sound from a rigid-wall turbulent boundary layer

Z.C. Zheng

Department of Mechanical and Nuclear Engineering, Kansas State University, Manhattan, KS 66506, USA

Received 19 January 2004; accepted 5 June 2004

Abstract

A theoretical model is developed to investigate the effect of compliant coatings on radiated sound from low Mach-number turbulent boundary layers over otherwise rigid surfaces. Lighthill's analogy is employed and the primary noise source is assumed to be from wall-pressure fluctuations. Parametric studies are performed on the behavior of the material properties such as the speed of sound and density of compliant coatings. Comparisons are made between the results from coated and uncoated rigid walls. At low frequencies, compliant coatings are not effective for noise reduction. At high frequencies, coating materials with low speed of sound and low density provide significant noise reduction.

1. Introduction

Compliant coatings on solid surfaces are expected to be able to reduce both drag and noise generated by flow over the surfaces. Effects of compliant coatings on drag reduction have been investigated during the last several decades [see review articles, e.g., Gad-el-Hak (1996, 1986)]. Most of the research is on using compliant coatings to delay the transition from a laminar to a turbulent boundary layer to reduce drag, and therefore these research works are based on laminar flow stability analysis [e.g., Yeo et al. (1999, 1994), Carpenter et al. (2001)]. For fully-developed turbulent boundary layers, detailed studies depend on direct numerical simulations. However, it is not feasible to simulate high Reynolds-number flow with the current or even near-future computational power. One tractable approach to tackle acoustic properties of turbulent boundary layers over compliant coatings is to make use of the Lighthill analogy (Lighthill, 1952, 1954; Ffowcs-Williams, 1965; Howe, 1984).

Using the Lighthill analogy, Zheng (2003) showed that for a two dimensional, nominally plane turbulent boundary layer, the pressure fluctuations could be determined by the Lighthill stress and the surface Green's function. In that analysis, the Lighthill stress was assumed to be the same as that in a turbulent boundary layer over a rigid surface; i.e., it used the weak coupling assumption (Graham, 1997; Zheng, 2003). This assumption is again adopted in the current study. Following the concept that the surface-property effect, due to either flexibility [as in Zheng (2003)] or compliancy (as in the current study), can be represented by a particular expression of the Green's function for each type of surface, a Green's function is constructed in this study that can represent properties of compliant coatings. Once the Green's function is determined, both the surface pressure and the far-field sound pressure can be expressed in terms of the

E-mail address: zzheng@ksu.edu (Z.C. Zheng).

0889-9746/$ - see front matter © 2004 Elsevier Ltd. All rights reserved.
doi:10.1016/j.jfluidstructs.2004.06.004

surface properties and the Lighthill stress. Comparisons then will be made between the results for walls with complaint coatings and those for rigid walls, in order to address the effect of compliant coatings. Effects on both the surface pressure fluctuations and the radiated sound are investigated. In order to facilitate theoretical comparisons, a wall-pressure correlation of Maestrello (1967) is used that will yield analytical expressions for radiated sound.

2. Preliminary formulation

For a low Mach number two-dimensional flat-plate boundary layer, Zheng (2003) showed that

$$p(x_1, x_2, t) = \int T_{ij} \frac{\partial^2 G}{\partial y_i \partial y_j} \, \mathrm{d}y_1 \, \mathrm{d}y_2 \, \mathrm{d}\tau, \tag{1}$$

where x and y are the coordinates in the radiation sound region and the source region, respectively, as illustrated in Fig. 1. The Lighthill stress tensor, T_{ij}, is expressed as

$$T_{ij} = \rho_o u_i u_j - e_{ij}, \quad e_{ij} = \mu_o \left(\frac{\partial u_i}{\partial x_j} + \frac{\partial u_j}{\partial x_i} - \frac{2}{3} \delta_{ij} \frac{\partial u_k}{\partial x_k} \right),$$

where u_i and p are the fluctuation components of velocity and pressure, respectively. The mean flow parameters, ρ_o, c_o and μ_o, are, respectively, the mean flow density, sound speed and viscosity. These flow properties are assumed to be constant in this problem. The Green's function, G, satisfies

$$\frac{1}{c_o^2} \frac{\partial^2 G}{\partial \tau^2} - \nabla^2 G = \delta(x_1 - y_1, x_2 - y_2, t - \tau), \tag{2}$$

with the boundary condition at $y_2 = 0$

$$\frac{\partial \hat{G}}{\partial y_2}(k_1, \omega) = \frac{\rho_o \omega^2 \hat{G}(k_1, \omega)}{Z(-k_1, -\omega)}, \tag{3}$$

where $Z(k_1, \omega)$ is the wall impedance based on displacement, and $\hat{f}$ is the Fourier transform of f defined as

$$\hat{f}(k_1, y_2, \omega) = \int_{-\infty}^{\infty} f(y_1, y_2, \tau) \mathrm{e}^{-\mathrm{i}(k_1 y_1 - \omega \tau)} \, \mathrm{d}y_1 \, \mathrm{d}\tau. \tag{4}$$

Eq. (1) shows that the fluctuation pressure is determined by the Lighthill stress T_{ij} and the Green's function G. The effect of wall-surface properties is entirely represented by the expression of G. That is because of the weak coupling assumption, as stated previously, that the Lighthill stress, T_{ij}, behaves the same as in a turbulent boundary layer over a rigid wall.

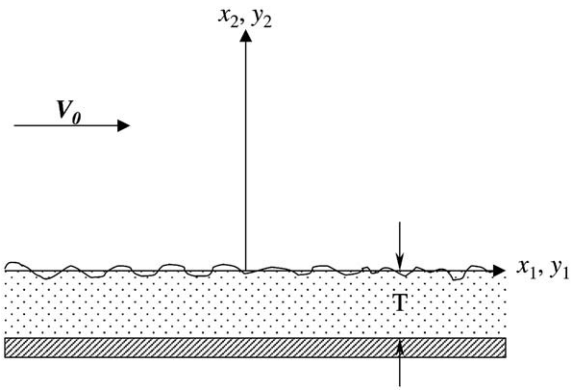

Fig. 1. Schematic illustration of the turbulent boundary flow over a surface coated by a compliant layer, and the coordinate system used in this study.

3. Effects of compliant coatings on wall-pressure fluctuations

Using Eq. (1) at the wall boundary (i.e. $x_2 = 0$), we have

$$p_w(x_1,t) = p(x_1,0,t) = \int T_{ij}\frac{\partial^2 G_{x_2=0}}{\partial y_i \partial y_j}\,\mathrm{d}y_1\,\mathrm{d}y_2\,\mathrm{d}\tau. \tag{5}$$

The Green's function at $x_2 = 0$ can be determined as (Zheng, 2003)

$$G_{x_2=0} = \frac{1}{(2\pi)^2}\int F(k_1,\omega)\mathrm{e}^{\mathrm{i}g}\mathrm{d}k_1\,\mathrm{d}\omega, \tag{6}$$

where

$$F(k_1,\omega) = \frac{Z(-k_1,-\omega)}{\rho_o\omega^2 + \mathrm{i}\gamma Z(-k_1,-\omega)}, \tag{7}$$

$$g = k_1(y_1 - x_1) - \omega(\tau - t) - \gamma y_2 \tag{8}$$

and

$$\gamma^2 = \frac{\omega^2}{c_o^2} - k_1^2. \tag{9}$$

For radiated sound, only $|k_1| < \omega/c_o$ is non-decaying; therefore γ is a positive real number (when $\omega > 0$). In the wavenumber-frequency domain, Eq. (5) thus reduces to

$$\hat{p}_w(k_1,\omega) = -\int F(-k_1,-\omega)(k_1\delta_{i1} - \gamma\delta_{i2}) \times (k_1\delta_{j1} - \gamma\delta_{j2})\mathrm{e}^{\mathrm{i}\gamma y_2}\hat{T}_{ij}\,\mathrm{d}y_2. \tag{10}$$

In Eq. (10), the effect of wall properties is reflected in different expressions for F based on different wall impedances, Z. On a rigid wall, because $Z \to \infty$, we have

$$F(-k_1,-\omega) = -\frac{1}{\mathrm{i}\gamma}. \tag{11}$$

On a wall coated with compliant materials, the impedance needs to be determined at the interface between the compliant coating and the fluid.

Consider a compliant layer illustrated in Fig. 1. The compliant layer is within the region of $-T \leqslant y_2 \leqslant 0$. In this compliant layer, it is assumed that the material particles only move in the vertical (y_2) direction, and that the horizontal (y_1) motion can be neglected. The propagation of fluctuations is in the form of a one-dimensional dilatation wave in the y_2 direction. By using the Euler equation of motion in a stationary elastic medium, the pressure fluctuation and the velocity fluctuation have a linear relationship given by

$$\rho_c\frac{\partial v_2}{\partial \tau} = -\frac{\partial p}{\partial y_2}, \tag{12}$$

where ρ_c is the density of the compliant layer. Let

$$v_2 = \frac{\partial \Psi}{\partial y_2}, \tag{13}$$

where Ψ is the velocity potential. Hence,

$$p = -\rho_c\frac{\partial \Psi}{\partial \tau}. \tag{14}$$

For the dilatation wave, the velocity potential satisfies

$$\frac{1}{c_d^2}\frac{\partial^2 \Psi}{\partial \tau^2} = \nabla^2\Psi, \tag{15}$$

where c_d is the dilatation wave speed or the speed of sound of the compliant layer. After taking the Fourier transform as defined in Eq. (4), the velocity potential can be determined as

$$\hat{\Psi} = C(k_1,\omega)\mathrm{e}^{\mathrm{i}\gamma_d y_2} - D(k_1,\omega)\mathrm{e}^{-\mathrm{i}\gamma_d y_2}, \tag{16}$$

where

$$\gamma_d = \frac{\omega^2}{c_d^2} - k_1^2 \tag{17}$$

and where C and D are the constants of integration. Substituting this solution into Eqs. (13) and (14), we have

$$\hat{v_2} = \mathrm{i}\gamma_d[C\mathrm{e}^{\mathrm{i}\gamma_d y_2} - D\mathrm{e}^{-\mathrm{i}\gamma_d y_2}] \tag{18}$$

and

$$\hat{p} = -\mathrm{i}\omega\rho_c[C\mathrm{e}^{\mathrm{i}\gamma_d y_2} + D\mathrm{e}^{-\mathrm{i}\gamma_d y_2}]. \tag{19}$$

On the rigid wall surface at $y_2 = -T$, we have $v_2 = 0$. Hence, from Eq. (18), it follows that

$$\frac{C}{D} = \mathrm{e}^{2\mathrm{i}\gamma_d T}. \tag{20}$$

Also from Eq. (18), the surface displacement at $y_2 = 0$ can be expressed as

$$\hat{\zeta}|_{y_2=0} = \frac{\gamma_d}{\omega}(C - D). \tag{21}$$

Therefore, the impedance at $y_2 = 0$ is

$$\begin{aligned} Z(k_1,\omega) = \frac{\hat{p}}{\hat{\zeta}}|_{y_2=0} &= \frac{-\mathrm{i}\omega\rho_c(C+D)}{\gamma_d/\omega(C-D)} \\ &= -\frac{\omega^2\rho_c}{\gamma_d}\cot(\gamma_d T). \end{aligned} \tag{22}$$

Substitution of Eq. (22) into Eq. (7) results in

$$F(-k_1,-\omega) = \frac{-(\rho_c/\gamma_d)\cot(\gamma_d T)}{\rho_o - (\mathrm{i}\gamma\rho_c/\gamma_d)\cot(\gamma_d T)}. \tag{23}$$

Now compare the surface-pressure fluctuations of a compliant wall with those of a rigid wall. For a rigid wall, which is the case in Eq. (23) with $T = 0$, we have

$$F(-k_1,-\omega) = -\frac{1}{\mathrm{i}\gamma}, \tag{24}$$

the same expression as Eq. (11). Eq. (24) can also be obtained from Zheng (2003) when the bending stiffness of a flexible wall becomes infinite (i.e., a rigid wall). Hence, according to Eq. (10), we can have

$$\begin{aligned} \frac{\hat{p}_{w\mathrm{rigid}}}{\hat{p}_{w\mathrm{compliant}}} &= \frac{F_{\mathrm{rigid}}(-k_1,-\omega)}{F_{\mathrm{compliant}}(-k_1,-\omega)} \\ &= 1 + \mathrm{i}\frac{\rho_o\gamma_d}{\rho_c\gamma}\tan(\gamma_d T). \end{aligned} \tag{25}$$

Now consider the magnitude of the ratio of the pressure fluctuations under the conditions that $c_d \leqslant c_o$ and $c_d > c_o$.

When $c_d \leqslant c_o$, then $\gamma_d^2 = \omega^2/c_d^2 - k_1^2 \geqslant \omega^2/c_o^2 - k_1^2 = \gamma^2 \geqslant 0$; therefore, the coefficient of the imaginary part of Eq. (25) is real and the magnitude of the ratio between the two pressure fluctuations in Eq. (25) is greater than one, except when

$$\gamma_d T = n\pi, \tag{26}$$

where n is a positive integer. Moreover, when ρ_o/ρ_c or c_o/c_d increases, the pressure fluctuation on the compliant wall decreases. When $|k_1|$ approaches ω/c_o, since $\gamma \to 0$, the reduction is significant because the compliant effect basically removes the singularity at $k_1 = \omega/c_o$ that occurs in the rigid wall case. This is no longer a singular point when a compliant surface is added to a rigid wall. When $|k_1| \ll \omega/c_o$, then

$$\frac{\rho_o\gamma_d}{\rho_c\gamma}\tan(\gamma_d T) \approx \frac{\rho_o c_o}{\rho_c c_d}\tan(\omega T/c_o). \tag{27}$$

That is, at high frequencies, the fluctuation-pressure reduction is proportional to the ratio of the characteristic impedances between the fluid and the compliant surface. The higher this ratio is, the greater the reduction that can be achieved.

When $c_d > c_o$, the case for $|k_1| \ll \omega/c_d$ is the same as $|k_1| \ll \omega/c_o$ in the previous case. However, when $\omega/c_d < |k_1| < \omega/c_o$, γ_d becomes imaginary. Therefore, Eq. (25) is rewritten as

$$\frac{\hat{p}_{w\text{rigid}}}{\hat{p}_{w\text{compliant}}} = 1 - \mathrm{i}\frac{\rho_o|\gamma_d|}{\rho_c\gamma}\tanh(|\gamma_d|T). \tag{28}$$

Eq. (28) shows that, in this case, the magnitude of the pressure fluctuation on the compliant surface is less than that on the rigid surface; hence, the compliant layer still has the noise-reduction effect. In particular, when ρ_o/ρ_c is bigger, the reduction effect is larger. In addition, since the tanh function only becomes zero when T is zero, exceptions at $\gamma_d T = n\pi$ no longer exist.

It should be noted that when ω is very small, the pressure-fluctuation-reduction effect of compliant coatings becomes insignificant because in both Eqs. (25) and (28) the coefficient of the imaginary part is small when ω is small.

4. Sound radiation from a rigid surface with a compliant layer

The power spectrum of radiated sound is defined as

$$P(\omega) = \int \langle p(x_1, x_2, t)p(x_1, x_2, t+\tau)\rangle \mathrm{e}^{\mathrm{i}\omega\tau}\,\mathrm{d}\tau, \tag{29}$$

where "$\langle\,\rangle$" denotes ensemble averages. If the convection effect from the turbulent boundary layer can be neglected and the surface-pressure fluctuation due to turbulence is a stationary random function, the power spectrum of radiated sound pressure can be expressed as (Tam, 1975)

$$P(\omega) = \frac{1}{(2\pi)^4}\int_{|k_1|<\omega/c_o} \hat{R}(k_1, \omega)\,\mathrm{d}k_1, \tag{30}$$

where the surface-pressure cross-correlation function, $\hat{R}(k_1, \omega)$, is expressed as

$$\hat{R}(k_1, \omega) = \int R(\xi, \eta)\mathrm{e}^{-\mathrm{i}(k_1\xi - \omega\eta)}\,\mathrm{d}\xi\,\mathrm{d}\eta \tag{31}$$

and

$$R(\xi, \eta) = \langle p_w(y_1', t')p_w(y_1'', t'')\rangle, \tag{32}$$

in which $\xi = y_1' - y_1''$ and $\eta = t' - t''$. For a compliant surface [or a flexible surface in Zheng (2003)], this surface-pressure cross-correlation function can be shown to be

$$\hat{R}(k_1, \omega) = \hat{R}_{\text{rigid}}(k_1, \omega)\gamma^2 F(-k_1, -\omega)F(k_1, \omega), \tag{33}$$

where $\hat{R}_{\text{rigid}}(k_1, \omega)$ is the surface-pressure cross-correlation function for a rigid surface. Therefore, substituting Eq. (23) into the above expression, we have

$$\hat{R}(k_1, \omega) = \hat{R}_{\text{rigid}}(k_1, \omega) - \frac{1}{1 + \left(\gamma^2\rho_c^2/\rho_o^2\gamma_d^2\right)\cot^2(\gamma_d T)} \times \hat{R}_{\text{rigid}}(k_1, \omega) \tag{34}$$

and Eq. (30) becomes

$$P(\omega) = P_{\text{rigid}}(\omega) - \frac{1}{(2\pi)^4}\int_{|k_1|<\omega/c_o} \frac{1}{1 + \left(\gamma^2\rho_c^2/\rho_o^2\gamma_d^2\right)\cot^2(\gamma_d T)} \times \hat{R}_{\text{rigid}}(k_1, \omega)\,\mathrm{d}k_1. \tag{35}$$

If γ_d is imaginary, the integrand in Eq. (35) can be re-written as

$$\frac{1}{1 + (\gamma^2\rho_c^2/\rho_o^2|\gamma_d|^2)\coth^2(|\gamma_d|T)}\hat{R}_{\text{rigid}}(k_1, \omega)\,\mathrm{d}k_1. \tag{36}$$

Because this integrand is positive definite, Eqs. (35) and (36) show that there is a reduced amount of the radiated sound spectrum from a compliant surface in comparison to that from a rigid surface.

For the purpose of quantitatively investigating the effect of compliant coatings, the experimental results of Maestrello (1967) are used for the wall-pressure cross-correlations, for the same reason as stated in Zheng (2003). The surface-pressure cross-correlation function for a rigid surface can then be expressed as (Zheng, 2003)

$$\hat{R}_{\text{rigid}}(k_1,\omega) = \frac{2\pi\bar{\tau}_w^2}{\left(U_c^2\theta/HU\right)\sum_{i=1}^{3}\frac{A_i}{\alpha_i}\left(\frac{\omega}{U_c}-k_1\right)^2+\left(1/U_c^2\theta^2\right)} \times \sum_{i=1}^{3} A_i \exp\left(-\alpha_i\frac{HU\omega}{U_c}\right), \tag{37}$$

where $\bar{\tau}_w$ is the mean-flow wall shear stress, A_i and α_i are the constants defined in Maestrello (1967), U is the freestream velocity, U_c is the convective velocity of eddies in the turbulent boundary layer (chosen as $0.8U$), and $H=\delta^*/U$ with $U_c\theta/\delta^*=17.0$, in which δ^* is the displacement thickness of the turbulent boundary layer. Substitution of Eq. (37) into Eq. (35) yields, in a dimensionless form,

$$\begin{aligned} LP &= \frac{P(\omega)(2\pi)^3}{H\bar{\tau}_w^2} = LP_{\text{rigid}} \\ &\quad - \frac{U/U_c}{\sum_{i=1}^{3}A_i/\alpha_i}\frac{QM}{U_c\theta/\delta^*}\sum_{i=1}^{3}A_i\exp\left(-\alpha_i Q\frac{U}{U_c}\right) \\ &\quad \times \int_{-1}^{1}\frac{1}{1+\left(\gamma^2\rho_c^2/\rho_o^2\gamma_d^2\right)\cot^2(\gamma_d T)} \\ &\quad \times \frac{\mathrm{d}y}{Q^2(U/U_c-My)^2+(U_c\theta/\delta^*)^{-2}}, \end{aligned} \tag{38}$$

where $y=k_1c_o/\omega$, $M=U/c_o$, and $Q=\delta^*\omega/U$. For LP_{rigid}, the following expression was obtained (Zheng, 2003):

$$\begin{aligned} LP_{\text{rigid}} &= \frac{P_{\text{rigid}}(\omega)(2\pi)^3}{H\bar{\tau}_w^2} \\ &= \frac{1}{\frac{U_c}{U}\sum_{i=1}^{3}A_i/\alpha_i}\left[\tan^{-1}\frac{2Q\left(U_c\theta/\delta^*\right)M}{1+Q^2\left(U_c\theta/\delta^*\right)^2\left(U^2/U_c^2-M^2\right)}\right] \\ &\quad \times \sum_{i=1}^{3}A_i\exp\left(-\alpha_i Q\frac{U}{U_c}\right). \end{aligned} \tag{39}$$

Again, there is a need to discuss separately the cases where $c_d \leqslant c_o$ and $c_d > c_o$.

For $c_d \leqslant c_o$, Eq. (38) can be expressed as

$$\begin{aligned} LP &= LP_{\text{rigid}} - \frac{U/U_c}{\sum_{i=1}^{3}A_i/\alpha_i}\frac{QM}{U_c\theta/\delta^*} \\ &\quad \times \sum_{i=1}^{3}A_i\exp\left(-\alpha_i Q\frac{U}{U_c}\right) \\ &\quad \times \int_{-1}^{1}\frac{1}{1+\left(1-y^2/(c_o/c_d)^2-y^2\right)\left(\frac{\rho_c}{\rho_o}\right)^2\cot^2\left(\sqrt{\left(\frac{c_o}{c_d}\right)^2-y^2}QM\frac{T}{\delta^*}\right)} \\ &\quad \times \frac{\mathrm{d}y}{Q^2(U/U_c-My)^2+(U_c\theta/\delta^*)^{-2}}. \end{aligned} \tag{40}$$

For $c_d > c_o$, Eq. (38) needs to be re-written as

$$LP = LP_{\text{rigid}} - \frac{U/U_c}{\sum_{i=1}^{3}A_i/\alpha_i}\frac{QM}{U_c\theta/\delta^*}\sum_{i=1}^{3}A_i\exp\left(-\alpha_i Q\frac{U}{U_c}\right)$$

$$\times \left\{ \int_{-c_o/c_d}^{c_o/c_d} \frac{1}{1+\left(1-y^2/(c_o/c_d)^2-y^2\right)\left(\frac{\rho_c}{\rho_o}\right)^2 \cot^2\left(\sqrt{\left(\frac{c_o}{c_d}\right)^2-y^2}QM\frac{T}{\delta^*}\right)} \right.$$

$$\times \frac{\mathrm{d}y}{Q^2(U/U_c-My)^2+(U_c\theta/\delta^*)^{-2}}$$

$$+ \int_{-1}^{-c_o/c_d} \frac{1}{1+\left(1-y^2/y^2-(c_o/c_d)^2\right)\left(\frac{\rho_c}{\rho_o}\right)^2 \coth^2\left(\sqrt{y^2-\left(\frac{c_o}{c_d}\right)^2}QM\frac{T}{\delta^*}\right)}$$

$$\times \frac{\mathrm{d}y}{Q^2(U/U_c-My)^2+(U_c\theta/\delta^*)^{-2}}$$

$$+ \int_{c_o/c_d}^{1} \frac{1}{1+\left(1-y^2/y^2-(c_o/c_d)^2\right)\left(\frac{\rho_c}{\rho_o}\right)^2 \coth^2\left(\sqrt{y^2-(\frac{c_o}{c_d})^2}QM\frac{T}{\delta^*}\right)}$$

$$\left. \times \frac{\mathrm{d}y}{Q^2(U/U_c-My)^2+(U_c\theta/\delta^*)^{-2}} \right\}.$$

In the following sample calculations, for the purpose of investigating the effect of related parameters, the physical properties are selected as: $c_d = c_o, 0.1c_o, 10c_o$; $\rho_c = \rho_o, 0.01\rho_o, 0.1\rho_o$. In all of the cases, it is assumed that $T/\delta^* = 1$ and the Mach number, M, is 0.1. The dimensionless frequency range is from 10^{-4} to 10. The numerical integrations in Eqs. (40) and (41) were obtained using the Romberg integration algorithm given in Press et al. (1986).

Fig. 2 shows the effect of the speed of sound of the compliant coating layer when $c_d \leqslant c_o$. The ratio of the speeds of sound between the compliant layer and the fluid, c_d/c_o, is specified as 1 and 0.1, to facilitate comparisons with the case of a rigid surface. The density ratio, ρ_c/ρ_o remains equal to unity. It can be seen that for the case of $c_d/c_o = 1$, there is basically no noise reduction. This is because, with $\rho_c = \rho_o$ and $c_d = c_o$, the compliant coating is basically the same material as the fluid as far as acoustic properties are concerned. For the case of $c_d/c_o = 0.1$, and at low frequencies where $\mathrm{Log}\, Q < -1.5$, there is still no noise reduction. However, at higher frequencies, significant decrease in the power

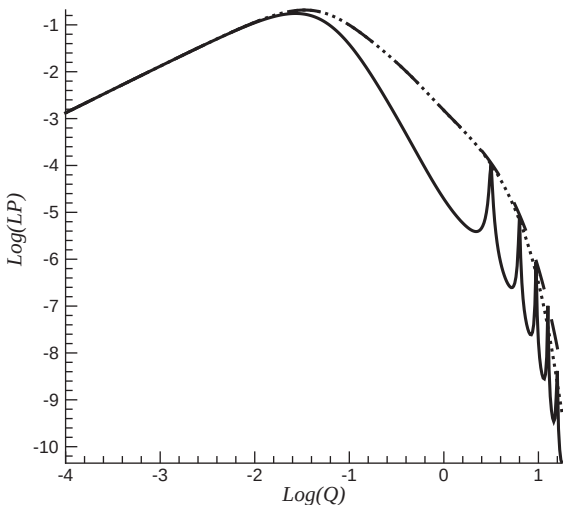

Fig. 2. Comparison of the effect of the speed-of-sound ratio of compliant coatings on radiated sound spectra when $c_d \leqslant c_o$. The dashed curve is for the rigid wall surface, the dotted curve is for the coated wall surface with $c_d = c_o$, and the solid curve is for the coated wall surface with $c_d = 0.1c_o$. The density ratio ρ_c/ρ_o is equal to 1.

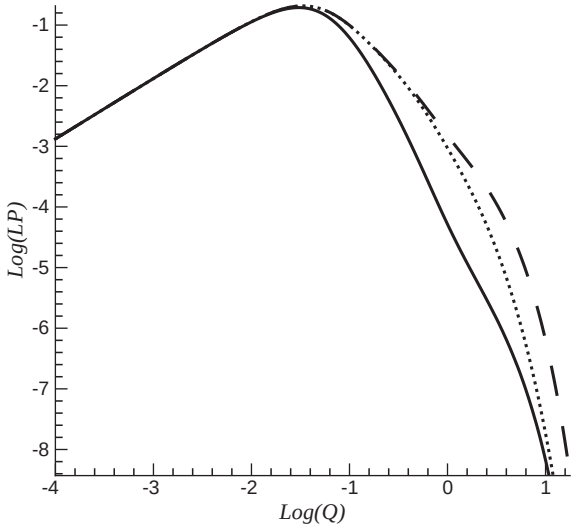

Fig. 3. Comparison of the effect of the density ratio of compliant coatings on radiated sound spectra. The dashed curve is for the rigid wall surface, the dotted curve is for the coated wall surface with $\rho_c/\rho_o = 0.1$, and the solid curve is for the coated wall surface with $\rho_c/\rho_o = 0.01$. The speed-of-sound ratio c_d/c_o is equal to 1.

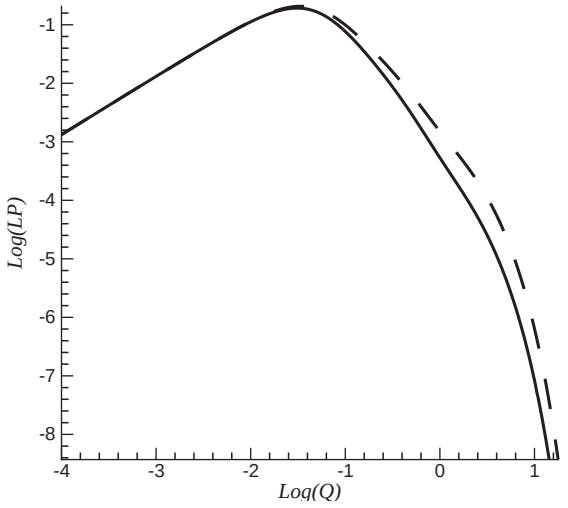

Fig. 4. Comparison of the effect of the speed-of-sound ratio of compliant coatings on radiated sound spectra when $c_d > c_o$. The dashed curve is for the rigid wall surface, and the solid curve is for the coated wall surface with $c_d = 10c_o$ and $\rho_c/\rho_o = 0.01$.

spectrum occurs, except at several spikes where the frequencies are close to the situation where

$$\frac{c_o}{c_d} QM \frac{T}{\delta^*} = \frac{\omega}{c_d} T = n\pi. \tag{42}$$

These are the same frequencies as those discussed in the wall-pressure case in the previous section for small k_1, i.e., as given in Eq. (26). In Eq. (40), when c_o/c_d is large (in this case it is equal to 10), the wave-number effect, represented by $y = k_1 c_o/\omega$, is small in the term involving $\sqrt{(c_o/c_d)^2 - y^2}$. This is because the y value for the radiated sound is between -1 and 1.

Fig. 3 is used to study the effect of the density of the compliant layer. The density ratio, ρ_c/ρ_o, is selected as 0.1 and 0.01 for comparison purposes, and c_d/c_o remains equal to 1. It can be seen that when ρ_c/ρ_c decreases, the noise reduction increases at high-frequency regimes. At low frequencies, no noise reduction is shown.

Fig. 4 is for the case where $c_d > c_o$, with $c_d = 10c_o$ and $\rho_c/\rho_o = 0.01$. It can be seen that there is still some noise reduction. In comparison with Fig. 3, however, the noise-reduction effect for $\rho_c/\rho_o = 0.01$ decreases due to the fact that the speed of sound of the compliant material is larger than that of the fluid.

The power spectra of radiated sound pressure from two-dimensional turbulent boundary layers over a rigid surface have been shown to be similar to those of the quadrupole sound radiation in this paper as well as in the literature [e.g., Blake (1986)]. Adding a compliant coating, however, does not change this basic shape of power spectra, unlike the effect of flexible walls that significantly alters the sound radiation power spectra of rigid walls (Vecchio and Wiley, 1973; Zheng, 2003). In all of the cases, no noise reduction is shown at low frequencies. This can be observed from the analytical expression of the power spectrum in Eq. (38). It can also be seen that, because the noise reduction part is proportional to the dimensionless frequency, Q, when Q is small, the reduction effect becomes small. This is the same type of frequency influence on the surface-pressure-fluctuation reduction as discussed in Section 3. Also as discussed in the previous section, the noise reduction of the compliant layer increases with ρ_o/ρ_c and c_o/c_d. This means that a compliant layer with lighter and more compressible materials seems to be a good sound muffling layer. In addition, Eq. (38) shows that the noise-reduction effect is proportional to the Mach number; but it should be noted that the expression is only valid for low Mach-number flow.

5. Conclusion

Once the surface impedance is found for an otherwise rigid surface with a compliant coating, the surface-pressure fluctuations under a turbulent boundary layer can be obtained using Lighthill's analogy. The power spectra of radiated noise based on the surface-pressure fluctuations are then calculated. In this theoretical model, several parameters are shown to influence the behavior of the noise-reduction effect of compliant coatings. Influential factors are the speed of sound and density of the coating material. Parametric studies have demonstrated that low speed of sound and low density of the coating material are effective in noise reduction. However, noise reduction barely exists in the low-frequency regime. At high frequencies, noise reduction of compliant coatings can be significant, except at frequencies where the thickness of the coating is equal to some of the multipliers of the sound wavelength of the material. Like any theory, the validity of the theoretical predictions in this paper is yet to be verified by future experimental results.

References

Blake, W.K., 1986. Mechanics of Flow-Induced Sound and Vibration, vols. 1 and 2. Academic Press, New York.

Carpenter, P.W., Lucey, A., Davies, C., 2001. Progress on the use of compliant walls for laminar-flow control. Journal of Aircraft 38, 504–512.

Ffowcs-Williams, J.E., 1965. Surface-pressure fluctuations induced by boundary-layer flow at finite Mach number. Journal of Fluid Mechanics 22, 507–519.

Gad-el-Hak, M., 1986. Boundary layer interactions with compliant coatings: an overview. Applied Mechanics Reviews 39, 511–523.

Gad-el-Hak, M., 1996. Compliant coatings: a decade of progress. Applied Mechanics Reviews 49, S147–S157.

Graham, W.R., 1997. A comparison of models for the wavenumber-frequency spectrum of turbulent boundary layer pressures. Journal of Sound and Vibration 206, 541–565.

Howe, M.S., 1984. On the production of sound by turbulent boundary layer flow over a compliant coating. IMA Journal of Applied Mathematics 33, 189–203.

Lighthill, M.J., 1952. On sound generated aerodynamically. I. General theory. Proceedings of the Royal Society of London A 211, 564–587.

Lighthill, M.J., 1954. On sound generated aerodynamically. II. Turbulence as a source of sound. Proceedings of the Royal Society of London A 222, 1–32.

Maestrello, L., 1967. Use of turbulent model to calculate vibration and radiation responses of panel, with practical suggestions for reducing sound level. Journal of Sound and Vibration 5, 407–448.

Press, W.H., Flannery, B.P., Teukolsky, S.A., Vetterling, W.T., 1986. Numerical Recipes. Cambridge University Press, New York, NY.

Tam, C.K.W., 1975. Intensity, spectrum, and directivity of turbulent boundary layer noise. Journal of the Acoustical Society of America 57, 25–34.

Vecchio, E.A., Wiley, C.A., 1973. Noise radiated from a turbulent boundary layer. Journal of the Acoustical Society of America 53, 596–601.

Yeo, K.S., Khoo, B.C., Chong, W.K., 1994. The linear stability of boundary-layer flow over compliant walls-the effects of the wall mean state, induced by flow loading. Journal of Fluids and Structures 8, 529–551.

Yeo, K.S., Khoo, B.C., Zhao, H.Z., 1999. The convective and absolute instability of fluid flow over viscoelastic wall. Journal of Sound and Vibration 223, 379–398.

Zheng, Z.C., 2003. Effects of flexible walls on radiated sound from a turbulent boundary layer. Journal of Fluids and Structures 18, 93–101.